Modulating magnetism of nitrogen-doped zigzag graphene nanoribbons*

Zhao Shang-Qian(赵尚骞)[a], Lü Yan(吕 燕)[a], Lü Wen-Gang(吕文刚)[a]†,
Liang Wen-Jie(梁文杰)[a], and Wang En-Ge(王恩哥)[b]

[a] *Institute of Physics, Chinese Academy of Sciences and Beijing National Laboratory for Condensed Matter Physics, Beijing* 100190, *China*
[b] *International Center for Quantum Materials, School of Physics, Peking University, Beijing* 100871, *China*

(Received 23 December 2013; revised manuscript received 10 March 2014; published online 20 April 2014)

We present a study of electronic properties of zigzag graphene nanoribbons (ZGNRs) substitutionally doped with nitrogen atoms at a single edge by first principle calculations. We find that the two edge states near the Fermi level separate due to the asymmetric nitrogen-doping. The ground states of these systems become ferromagnetic because the local magnetic moments along the undoped edges remain and those along the doped edges are suppressed. By controlling the charge-doping level, the magnetic moments of the whole ribbons are modulated. Proper charge doping leads to interesting half-metallic and single-edge conducting ribbons which would be helpful for designing graphene–nanoribbon-based spintronic devices in the future.

Keywords: graphene nanoribbons, charge doping, spin-polarization, spatial localization

PACS: 73.22.Pr, 75.75.–c, 71.15.Mb **DOI:** 10.1088/1674-1056/23/6/067305

1. Introduction

Graphene, which is a single layer of graphite, has attracted tremendous attention since its first isolation by K. S. Novoselov and A. K. Geim in 2004.[1,2] Due to its fascinating physical properties, especially its potential applications in nanoelectronics and spintronics, researchers have made great efforts to work on it and its related materials.[3–7] Graphene nanoribbons (GNRs), which can be seen as ribbons cut from graphene,[8–11] show more interesting properties because of the further confinement and the new emerging edge states. According to the edge shapes of GNRs, there are two typical kinds of graphene nanoribbons: zigzag graphene nanoribbons (ZGNRs) and armchair graphene nanoribbons (AGNRs). The edge states of ZGNRs bring about flat dispersion subbands near the Fermi level and cause the magnetic ordering states at the edge atoms,[12,13] which can be used as separate spin channels for spin-polarized quantum transports.[14,15] Thus, ZGNRs have become important candidates for the next generation of spintronic devices, and attracted a lot of attention both in experimental and theoretical research.

Substitutional doping is a promising way to modulate the electronic and magnetic properties of ZGNRs. Scientists have realized experimentally the substitutional doping with nitrogen atoms in GNRs.[16] Simultaneously, some theoretical works have been done on the effects of nitrogen or boron doping in ZGNRs.[17–26] Much interesting physics has been obtained, such as the half-metallic behavior,[18] the spin gapless semiconducting behavior,[19] and the spin-polarized quantum transport.[25,26] Besides, previous investigations have shown that the dopants locate preferably at the edges of ZGNRs.[17,19,21–24] It has also been demonstrated that edge impurities can suppress the spin polarizations at the doped edges.[19,20] Although the suppression of the local spin moments at the doped edges have been reported by several works, further studies are still necessary to fully understand and precisely control magnetic configurations of edge states for practical applications in spintronic devices.

In this paper, we will construct a ZGNR and substitutionally dope it by nitrogen atoms only at a single edge. The edge states are spin-polarized when they are shifted to the Fermi level through charge doping, which can be explained by the Stoner model for sp electrons forming a narrow band to render instability of spin splitting.[27–29] In practice, charge doping can be achieved by putting the samples on proper substrates[28–32] or applying a gate voltage.[33–35] We will also systematically discuss the change of the total magnetic moment of the whole ribbon and the distribution of the local magnetic moments in the ribbon. Results demonstrate that the direction and the spatial localization of the magnetic moment of this system are tunable via electrical methods. Besides, spatially-localized half-metallic states can be realized by modulating charge-doping level properly.

2. Computational methods

The first principle calculations are carried out by using the Vienna *ab initio* simulation package (VASP)[36–38] with a

*Project supported by the National Natural Science Foundation of China (Grant Nos. 10834012 and 11374342), National Key Basic Research and Development Program of China (Grant No. 2009CB930700), and the Knowledge Innovation Foundation of the Chinese Academy of Sciences (Grant No. KJCX2-YW-W35).

†Corresponding author. E-mail: wglu@iphy.ac.cn

© 2014 Chinese Physical Society and IOP Publishing Ltd

plane-wave-kinetic cutoff energy of 550 eV. The exchange–correlation is approximated by the Perdew–Burke–Ernzernhof (PBE)[39] generalized gradient approximation (GGA) both for spin-unpolarized and spin-polarized cases. The pseudopotential of the core electrons are described by the projector augmented wave (PAW) method.[40,41] A $9 \times 1 \times 1$ gamma-centered k mesh and Gaussian method with a smearing width of 0.1 eV are employed for the structure optimizations and the static self-consistent calculations. Denser k meshes are used to obtain the electronic structures and the density of states. For all the calculations, the atomic positions are relaxed sufficiently and the force tolerance is set to be 0.01 eV/Å. In our calculations, the supercells are periodic along the ribbon direction X. The thicknesses of the vacuum region inserted in two neighboring images in the Y and Z directions are about 2 nm, which are large enough to avoid interactions.

3. Results and discussion

3.1. Single-edge nitrogen doping

3.1.1. Spin-unpolarized case

Figure 1(a) shows the optimized atomic structure of an undoped ZGNR with $W = 4$, where W is the number of the zigzag lines along the ribbon. Here the C and H atoms are shown in black and light pink colors respectively. Figures 1(b) and 1(c) present the spin-unpolarized band structure and the density of states (DOS) of the pristine ZGNR. Note that the supercell unit we used for the pristine ZGNR is three times that of the primitive cell's. The flat subbands (in magenta) near the Fermi level originate from the edge states localized at the two edges and cause a sharp DOS peak close to the Fermi level. Figure 1(d) shows the isosurface of the partial charge densities of the subbands marked by magenta color in Fig. 1(b), which demonstrates their edge-localized characters.

Figure 2(a) shows a supercell of a single-edge nitrogen-doped ZGNR with $W = 4$. The doping is achieved by substituting a single carbon (C) atom at one edge with a nitrogen (N) atom in every three units. Here N atom is shown in green color. After relaxation, the C–N and N–H bond lengths are 1.389 Å and 1.015 Å respectively, which are smaller than the C–C bond length of 1.407 Å at the edge and the C–H bond length of 1.093 Å for the pristine ZGNRs respectively. All the atoms are still in the same plane after relaxation. The influence of the N-substitutional doping upon the band structure and the DOS are shown in Figs. 2(b) and 2(c). The most distinct difference after doping is the separation of the edge subbands with an energy gap of 0.92 eV. The upper edge subband marked with the red arrow relates to the edge states localized at the undoped edge, while the lower one marked with the blue arrow relates to the edge states localized at the doped edge, which are confirmed by their partial-charge-density contours plotted in Figs. 2(d) and 2(e), corresponding to the red-arrow-marked and the blue-arrow-marked subbands respectively. Thus, these two subbands are edge states localized along the undoped edge and the N-doped edge respectively.

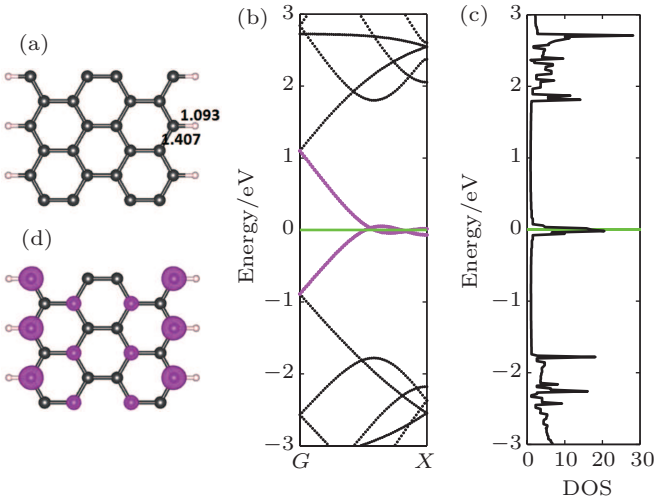


Fig. 1. (color online) (a) A supercell of a pristine ZGNR with $W = 4$. The C–C and the C–H bond lengths are 1.407 Å and 1.093 Å respectively. Panels (b) and (c) are the spin-unpolarized band structure and the density of states of the pristine ZGNR. The green lines indicate the positions of the Fermi levels. The magenta subbands are edge states, whose partial-charge-density contours are shown in panel (d).[42] The magenta surfaces in panel (d) represent the isovalues of 0.01 e/a_0^3 (a_0: Bohr radius).

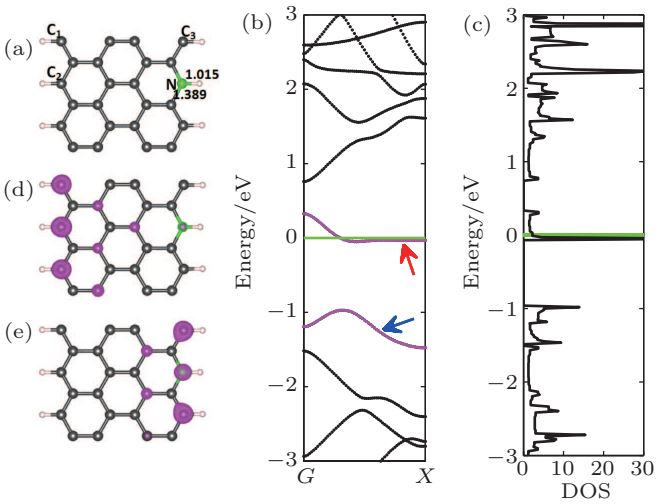


Fig. 2. (color online) (a) A supercell of an N-doped ZGNR with $W = 4$. The C–N and the N–H bond lengths are 1.389 Å and 1.015 Å respectively. Panels (b) and (c) are the spin-unpolarized band structure and density of states of the N-doped ZGNR, respectively. Panels (d) and (e) show the partial-charge-density contours of the magenta subbands marked by the red and the blue arrows in panel (b), respectively. The magenta surfaces in panels (d) and (e) represent the isovalues of 0.01 e/a_0^3 (a_0: Bohr radius).

3.1.2. Spin-polarized case

When spin degree is taken into consideration, edge states of the pristine ZGNR in Fig. 1(a) split into different spins and a small band gap appears, as shown in Figs. 3(a) and 3(b).

The local magnetic moments emerge at the two edges and the ground state of the magnetic configuration is ferromagnetic on each edge and antiferromagnetic between the two opposite edges which is illustrated in Fig. 3(c). Besides, the total magnetic moment of the system remains zero. All of these are consistent with previous works.[12,13] The emergence of the energy gap and the local magnetism can be understood and explained by the Stoner model for sp electrons[27,28] as follows. If the Stoner criterion for ferromagnetism, $I_{\rm eff}N(E_{\rm F}) > 1$,[43] (see Appendix A for details), is satisfied, the spin-degenerate states near the Fermi level will split apart due to the spin-exchange interactions. Here $N(E_{\rm F})$ is the density of one-electron states at the Fermi level in the paramagnetic state and $I_{\rm eff}$ is an on-site interaction parameter. For the pristine ZGNR, the flat edge states localized along the two edges have a sharp DOS near the Fermi level [see in Fig. 1(c)], which satisfies the Stoner criterion.

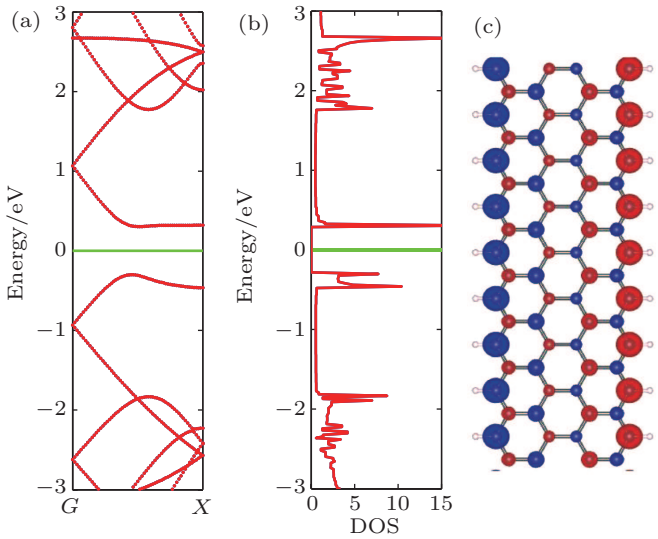


Fig. 3. (color online) (a) Spin-resolved band structure, (b) total density of states and (c) isosurface of the spin charge density of the pristine ZGNR [Fig. 1(a)] when spin degree is taken into consideration. Here the spin charge density equals $\rho_\uparrow - \rho_\downarrow$, where $\rho_\uparrow$ and $\rho_\downarrow$ are the charge densities of the spin-up and the spin-down electrons respectively. The blue and red surfaces in panel (c) represent the isovalues of 0.004 e/a_0^3 and -0.004 e/a_0^3, respectively (a_0: Bohr radius). The same characterization methods are used throughout the rest of this paper.

Similar to the pristine ZGNR [Fig. 1(a)], the doped one [Fig. 2(a)] also has a sharp DOS peak near the Fermi level, as shown in Fig. 2(c). This peak corresponds to the edge state at the undoped edge, and leads to instability when spin-exchange interaction is taken into account. Figures 4(a) and 4(b) show the spin-polarized band structure and the DOS of the ground magnetic state which is about 74 meV lower than the spin-unpolarized ground state. The subbands localized at the two edges are plotted in bold for clarity. The blue and the red lines represent the spin-up and the spin-down bands respectively. The sharp DOS peak in Fig. 2(c) makes the Stoner criterion more easily satisfied. Here in Figs. 4(a) and 4(b), the large separation of the spin-subbands near the Fermi level indicates that the Stoner criterion has actually been obeyed. The spin splitting of the edge states localized at the undoped edge causes the spin polarization and the local magnetic moments at this edge. Because both the spin states localized at the doped edge are below the Fermi level and occupied, the spin polarization and the local magnetization of this edge are suppressed, which are consistent with previous investigations.[19,20] So the undoped and the doped edges are ferromagnetic and nonmagnetic respectively and therefore the doped ZGNR has a ferromagnetic ground state with a total magnetic moment of $\mu = 0.77$ $\mu_{\rm B}$. The isosurface of the spin charge density (magnetization density) is plotted in Fig. 4(c).

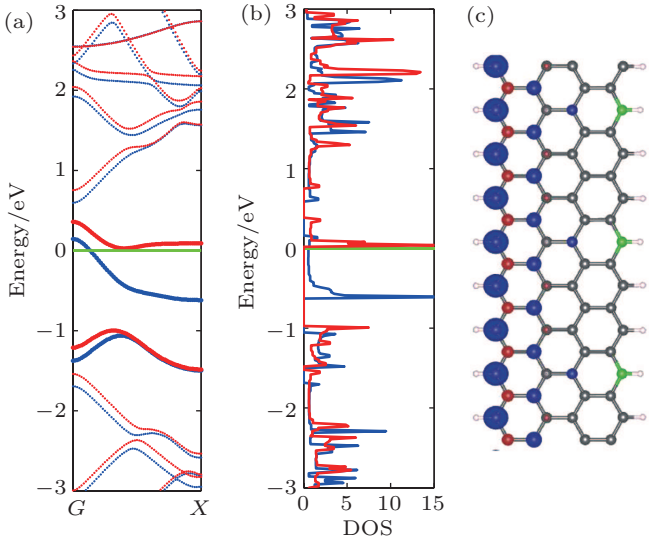


Fig. 4. (color online) (a) Spin-polarized band structure, (b) total density of states, and (c) isosurface of the spin charge density of the single-edge-N-doped ZGNR [Fig. 2(a)] at neutral states with $\Delta e = 0$ e. Here Δe represents the change of valance electrons per supercell. Blue and red colors in panels (a) and (b) represent spin-up and spin-down respectively. Bold lines in panel (a) are used to highlight the two edge-subbands.

3.2. Charge doping effect

The charge doping can be realized by metal substrates or nearby electrostatic centers.[28–32] It can also be achieved by applying a gate voltage on purpose.[33–35] Generally, gate voltage changes the number of electrons in a conductor through electrostatic interaction.

In our calculations, the number of electrons in the supercell are changed starkly to simulate the effect of charge doping.[44,45] For the single-edge-N-doped ZGNR shown in Fig. 2(a), there are 23 C, 6 H, and 1 N atoms in one supercell. The 2s and 2p orbitals of the C and N atoms are treated as valence electrons. So there are 103 valence electrons in one supercell. Δe is used to represent the change of the valence electrons per supercell. Positive Δe means that electrons are added into the system, which simulates the effect of a positive

gate voltage (electron doping). Negative Δe means that electrons are extracted from the system, which simulates the effect of a negative gate voltage (hole doping).

In the above discussion of $\Delta e = 0$ e, the subband of the undoped edge near the Fermi level splits, and the spin polarization induces the ferromagnetically coupled local magnetic moments at this edge [Fig. 4]. When Δe changes to -1 e, the Fermi level shifts downward and the subband localized at the undoped edge moves away from the Fermi level, which leads to weaker satisfaction of the Stoner criterion for this subband. Here, weaker satisfaction means the Stoner criterion is satisfied with a reduction of $N(E_F)$. Therefore, this subband does not split as much as that of $\Delta e = 0$ e. The splitting energy gap of this subband reduces from 0.71 eV to 0.12 eV at the X point and the local spin moments at the undoped edge almost disappear, as shown in Fig. 5. Accordingly, the total magnetic moment of the supercell reduces to 0.07 μ_B.

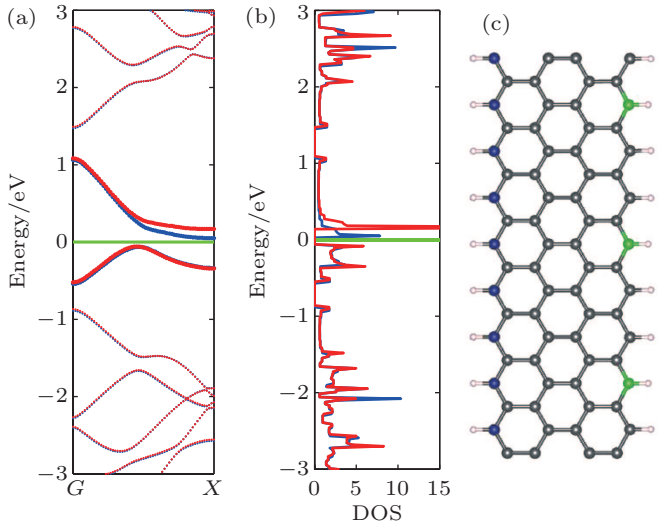


Fig. 5. (color online) (a) Spin-polarized band structure, (b) total density of states, and (c) isosurface of the spin charge density for the single-edge-N-doped ZGNR [Fig. 2(a)] with $\Delta e = -1$ e.

When Δe changes -2 e, the spin-configuration of $\Delta e = -1$ e is used as the initial values for the next self-consistent calculations. The electronic structure in Fig. 6(a) indicates that the subband at the undoped edge moves far away from the Fermi level and splits little, which leads to the suppression of the local spin moments of the undoped edge. However, the flat subband from the N-doped edge moves closer to the Fermi level, so that the Stoner criterion is preferably satisfied due to the existence of the sharp DOS peak. It becomes almost totally spin-polarized with an energy gap of 0.62 eV at the X point [Figs. 6(a) and 6(b)], which leads to the emergence of the local magnetic moments at the doped edge, as shown in Fig. 6(c). The total magnetic moment of the system is -0.82 μ_B. It should be pointed out that the direction of the magnetic moment of $\Delta e = -2$ e [Fig. 6(c)] is opposite to that of $\Delta e = 0$ e [Fig. 4(c)], i.e., the spin-up and the spin-down charges prevail respectively in these two cases. Besides, not only the magnetization direction but also the distribution of the local magnetic moments are controlled by charge doping.

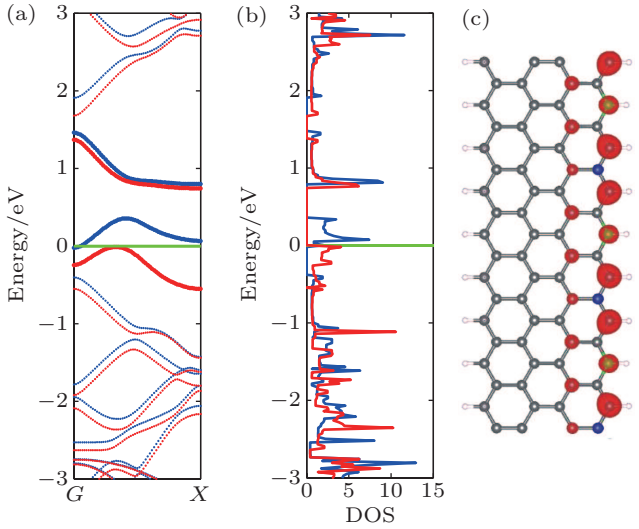


Fig. 6. (color online) (a) Spin-polarized band structure, (b) total density of states, and (c) isosurface of the spin charge density for the single-edge-N-doped ZGNR [Fig. 2(a)] with $\Delta e = -2$ e.

The reason for the flipping of the magnetic-moment direction can be understood as follows. During the charge-doping process from $\Delta e = 0$ e to $\Delta e = -2$ e, the local magnetic moments at the undoped edge keep decreasing. But before the local magnetic moments at the undoped edge become zero, small magnetic moments with opposite direction have already emerged at the doped edge. For example, the total magnetic moment for $\Delta e = -1$ e almost equals zero, but it has weak spin-up charges at the undoped edge and weak spin-down charges at the doped edge simultaneously [this cannot be directly viewed in Fig. 5(c) due to the small values of the local magnetic moments]. With the further increase of charge doping, the local magnetic moments at the doped edge with opposite direction keep increasing, and the total magnetic moment begins to appear with the opposite direction. Thus, the flipping of magnetic-moment direction is realized.

When Δe equals -3 e, the Fermi level moves downward further. As shown in Figs. 7(a) and 7(b), the subband from the doped edge also moves away from the Fermi level. Therefore, the splitting of this edge subband also reduces due to weaker satisfaction of the Stoner criterion. The splitting energy gap of this edge subband is decreased to 0.25 eV at the X point in this case. As illustrated in Fig. 7(c), the local spin moments of the doped edge are suppressed to a certain degree compared with Fig. 6(c). Besides, the total magnetic moment reduces to -0.21 μ_B.

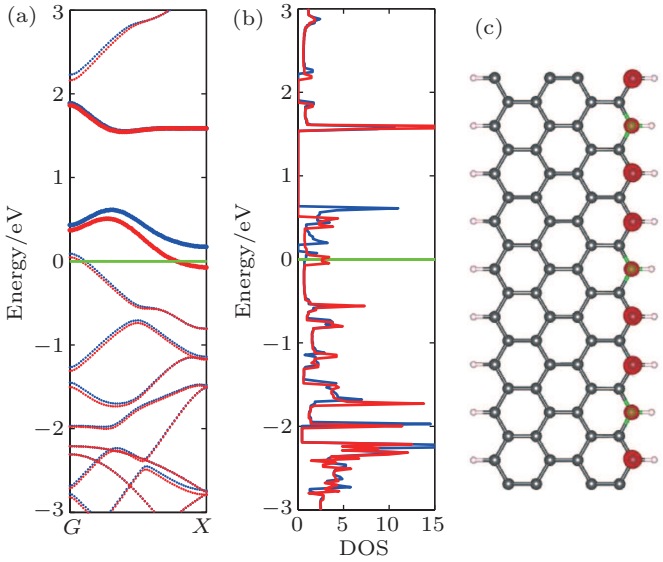


Fig. 7. (color online) (a) Spin-polarized band structure, (b) total density of states, and (c) isosurface of the spin charge density for the single-edge-N-doped ZGNR [Fig. 2(a)] with $\Delta e = -3$ e.

In order to illustrate the change of the magnetic configuration with charge-doping level clearly, the total magnetic moment and the local magnetic moments of the edge atoms as a function of Δe are plotted in Figs. 8(a) and 8(b) respectively. In Fig. 2(a), the representative edge carbon atoms are labeled by C_1, C_2, C_3, and the nitrogen atom is labeled by N. The total magnetic moment changes greatly with the charge-doping level as shown in Fig. 8(a). It changes from a positive value of 0.77 μ_B at $\Delta e = 0$ e to almost 0 μ_B at $\Delta e = -1$ e and then to a negative value of -0.82 μ_B at $\Delta e = -2$ e, which means that the total magnetic moment can be quenched and its direction can be flipped merely by charge doping. With further doping, the total magnetic moment decreases again to -0.21 μ_B at $\Delta e = -3$ e due to the reduction of the spin-splitting of the subband from the doped edge. When $\Delta e < -3$ e, both of the edge-subbands are far away from the Fermi level. As a result, no Stoner instability occurs, and the total magnetic moment remains at 0 μ_B. The local spin moments of the edge atoms contribute a large amount to the total magnetic moment. Figure 8(b) shows that along with the change of the doping level, the local magnetic moments of the atoms at the undoped edge, C_1 and C_2, and at the doped edge, C_3 and N, show different changing modes, which are consistent with the change of spin charge density distribution with Δe.

In addition, proper charge-doping levels can exhibit more interesting half-metallic behaviors, as shown in Figs. 9(a) and 9(c), where Δe equals -0.2 e and -2.4 e respectively. When $\Delta e = -0.2$ e, it is metallic for spin-up electrons and insulating for spin-down electrons. The electrons in the spin-up subband crossing the Fermi level localize along the undoped edge as shown in Fig. 9(b). However, when Δe turns to -2.4 e, it is metallic for spin-down electrons and insulating for spin-up electrons, and the electrons in the spin-down subband crossing the Fermi level localize along the doped edge as shown in Fig. 9(d). Since it is the subband across the Fermi level that determines the electronic transport properties, the spin-polarized and the spatially-localized current simultaneously occur in the single-edge-N-doped graphene for $\Delta e = -0.2$ e or $\Delta e = -2.4$ e. These interesting results may be useful in the application of spintronics in the future.

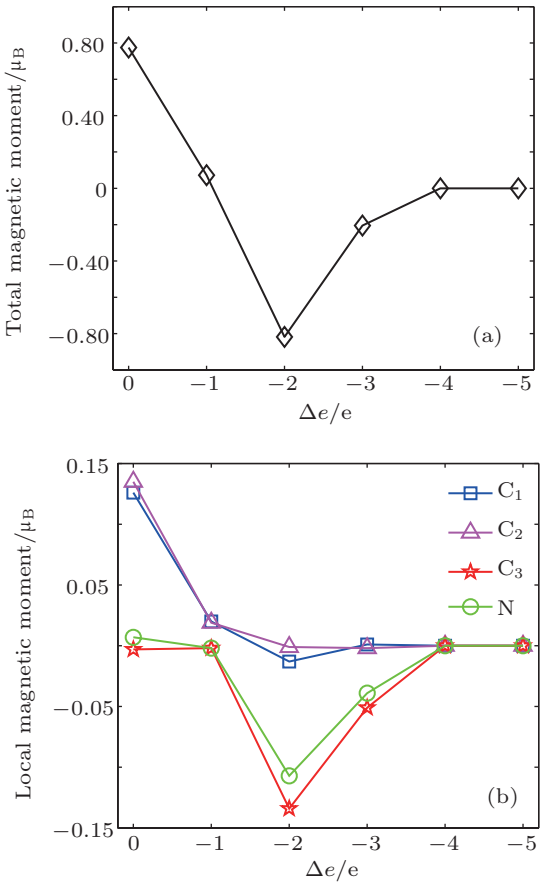


Fig. 8. (color online) (a) Total magnetic moments and (b) local magnetic moments as a function of Δe. The edge atoms C_1, C_2, C_3, and N are labeled in Fig. 2(a). The positive and negative signs of the magnetic moments represent their directions.

Similar to the discussion about $\Delta e < 0$ e, we can also discuss the case for $\Delta e > 0$ e, simulating electron doping. In this case, the Fermi energy shifts upward. The local spin moments at the doped edge are zero, because the subband localized at the doped edge is always far away from the Fermi energy. Also, the subband localized at the undoped edge moves away from the Fermi energy with the doping level, which leads to weaker satisfaction of the Stoner criterion. Thus, with the increasing of electron doping levels, the local magnetic moments at the undoped edge and the total magnetic moment tend to be suppressed.

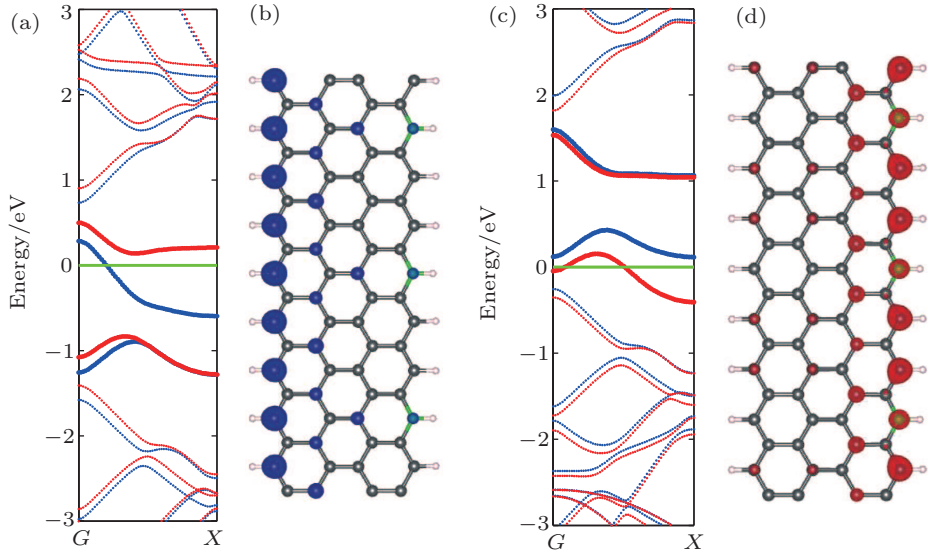


Fig. 9. (color online) Spin-polarized band structures and partial charge densities of subbands across the Fermi level for $\Delta e = -0.2\ e$ [panels (a) and (b)] and $\Delta e = -2.4\ e$ [panels (c) and (d)]. Half-metallic behaviors are obtained because of the spin-up subband crossing the Fermi level in panel (a) and the spin-down subband crossing the Fermi level in panel (c). Besides, the electrons in the subbands crossing the Fermi level in panels (a) and (c) localize at different edges, as shown in panels (b) and (d) respectively.

The above results show that the electronic and magnetic properties of N-doped ZGNRs can be tuned by charge doping. This is consistent with previous theoretical investigations on ZGNRs and other graphene-based materials.[44,45] For example, the edge magnetism of ZGNRs can become significantly weak and even vanishing as the charge doping level increases.[44] Experimentally, it has been demonstrated that the properties of graphene-based materials can deviate from the neutral states due to the charge doping.[46–49]

4. Conclusion

In conclusion, the electronic properties of ZGNRs with single-edge N-doping have been studied through first principle calculations. The two edge-states on the two opposite edges of the pristine ZGNR with $W = 4$ will separate due to the asymmetric nitrogen-doping. When spin polarization is taken into account, the local magnetic moments are ferromagnetically coupled at the undoped edge, and they are quenched at the doped edge. By charge-doping, the Fermi level moves from one edge-subband to the neighborhood of the other edge-subband. Along with that, the local magnetic moments at the undoped edge fade out and those at the doped edge emerge gradually with the opposite magnetic moment direction. At the same time, the total magnetic moment of the system decreases first, then changes its direction and increases its value. All these phenomena can be understood by the Stoner criterion. Our study shows the interesting results of modulating the total and local magnetic moments of N-doped ZGNRs through charge doping, which is enlightening for the application of graphene-based materials in spintronic devices.

Appendix A

The Stoner criterion can be understood from the view of energy balance for the ferromagnetic order.[43] When spin-down electrons with energies from $E_F - \delta E$ up to E_F flip their spins and fill in spin-up band with energies from E_F up to $E_F + \delta E$, the increase of kinetic energy $\Delta E_{K.E.}$ equals to $\frac{1}{2}N(E_F)(\delta E)^2$, where $N(E_F)$ is the density of one-electron states at the Fermi level in the paramagnetic state. Simultaneously, the interaction of the magnetization M with the molecular field gives an energy reduction of

$$\begin{aligned}\Delta E_{M.E.} &= -\int_0^M \mu_0(\lambda M')\,\mathrm{d}M' = -\frac{1}{2}\mu_0\lambda M^2 \\ &= -\frac{1}{2}\mu_0\mu_B^2\lambda(n_\uparrow - n_\downarrow)^2.\end{aligned}$$

Here μ_0 is the permeability of free space and λ is a constant which parameterizes the strength of the molecular field as a function of the magnetization. The number density of up-spins $n_\uparrow$ equals $\frac{1}{2}(n + N(E_F)\delta E)$ and the number density of down-spins $n_\downarrow$ equals $\frac{1}{2}(n - N(E_F)\delta E)$. Writing $I_{eff} = \mu_0\mu_B^2\lambda$, we have $\Delta E_{M.E.} = -\frac{1}{2}I_{eff}(N(E_F)\delta E)^2$. Hence the total change of energy is $\triangle E = \Delta E_{K.E.} + \Delta E_{M.E.} = \frac{1}{2}N(E_F)(\delta E)^2(1 - I_{eff}N(E_F))$. Thus spontaneous ferromagnetism is energetically favorable when $I_{eff}N(E_F) > 1$.

References

[1] Novoselov K S, Geim A K, Morozov S V, Jiang D, Zhang Y, Dubonos S V, Grigorieva I V and Firsov A A 2004 *Science* **306** 666
[2] Novoselov K S, Geim A K, Morozov S V, Jiang D, Katsnelson M I, Grigorieva I V, Dubonos S V and Firsov A A 2005 *Nature* **438** 197
[3] Castro Neto A H, Guinea F, Peres N M R, Novoselov K S and Geim A K 2009 *Rev. Mod. Phys.* **81** 109
[4] Terrones H, Lü R, Terrones M and Dresselhaus M S 2012 *Rep. Prog. Phys.* **75** 062501

[5] Abergel D S L, Apalkov V, Berashevich J, Ziegler K and Chakraborty T 2010 *Adv. Phys.* **59** 261
[6] Yazyev O V 2010 *Rep. Prog. Phys.* **73** 056501
[7] Andrei E Y, Li G H and Du X 2012 *Rep. Prog. Phys.* **75** 056501
[8] Han M Y, Özyilmaz B, Zhang Y B and Kim P 2007 *Phys. Rev. Lett.* **98** 206805
[9] Li X L, Wang X R, Zhang L, Lee S and Dai H J 2008 *Science* **319** 1229
[10] Wang X R, Ouyang Y J, Li X L, Wang H L, Guo J and Dai H J 2008 *Phys. Rev. Lett.* **100** 206803
[11] Shi Z W, Yang R, Zhang L C, Wang Y, Liu D H, Shi D X, Wang E G and Zhang G Y 2011 *Adv. Mater.* **23** 3061
[12] Son Y W, Cohen M L and Louie S G 2006 *Nature* **444** 347
[13] Son Y W, Cohen M L and Louie S G 2006 *Phys. Rev. Lett.* **97** 216803
[14] Wimmer M, Adagideli İ, Berber S, Tománek D and Richter K 2008 *Phys. Rev. Lett.* **100** 177207
[15] Wang B, Wang J and Guo H 2009 *Phys. Rev. B* **79** 165417
[16] Wang X R, Li X L, Zhang L, Yoon Y K, Weber P K, Wang H L, Guo J and Dai H J 2009 *Science* **324** 768
[17] Biel B, Blase X, Triozon F and Roche S 2009 *Phys. Rev. Lett.* **102** 096803
[18] Zheng X H, Wang X L, Abtew T A and Zeng Z 2010 *J. Phys. Chem. C* **114** 4190
[19] Li Y F, Zhou Z, Shen P W and Chen Z F 2009 *ACS Nano* **3** 1952
[20] Huang B, Liu F, Wu J, Gu B L and Duan W H 2008 *Phys. Rev. B* **77** 153411
[21] Cruz-Silva E, Barnett Z M, Sumpter B G and Meunier V 2011 *Phys. Rev. B* **83** 155445
[22] Yu S S, Zheng W T, Wen Q B and Jiang Q 2008 *Carbon* **46** 537
[23] Jiang J, Turnbull J, Wen W C, Boguslawski P and Bernholc J 2012 *J. Chem. Phys.* **136** 014702
[24] Xiao J, Yang Z X, Xie W T, Xiao L X, Xu H and Ouyang F P 2012 *Chin. Phys. B* **21** 027102
[25] Martins T B, Miwa R H, da Silva A J R and Fazzio A 2007 *Phys. Rev. Lett.* **98** 196803
[26] Martins T B, da Silva A J R, Miwa R H and Fazzio A 2008 *Nano Lett.* **8** 2293
[27] Edward D M and Katsnelson M I 2006 *J. Phys.: Condens. Matter* **18** 7209
[28] Chen J Z, Vanin M, Hu Y B and Guo H 2012 *Phys. Rev. B* **86** 075146
[29] Li Y, Zhang W, Morgenstern M and Mazzarello R 2013 *Phys. Rev. Lett.* **110** 216804
[30] Giovannetti G, Khomyakov P A, Brocks G, Karpan V M, van den Brink J and Kelly P J 2008 *Phys. Rev. Lett.* **101** 026803
[31] Khomyakov P A, Giovannetti G, Rusu P C, Brocks G, van den Brink J and Kelly P J 2009 *Phys. Rev. B* **79** 195425
[32] Shim J, Lui C H, Ko T Y, Yu Y J, Kim P, Heinz T F and Ryu S 2012 *Nano Lett.* **12** 648
[33] Meric I, Han M Y, Young A F, Ozyilmaz B, Kim P and Shepard K L 2008 *Nat. Nanotech.* **3** 654
[34] Xia F N, Farmer D B, Lin Y M and Avouris P 2010 *Nano Lett.* **10** 715
[35] Liao L, Lin Y C, Bao M Q, Cheng R, Bai J W, Liu Y, Qu Y Q, Wang K L, Huang Y and Duan X F 2010 *Nature* **467** 305
[36] Kresse G and Hafner J 1993 *Phys. Rev. B* **48** 13115
[37] Kresse G and Furthmüller J 1996 *Comput. Mater. Sci.* **6** 15
[38] Kresse G and Furthmüller J 1996 *Phys. Rev. B* **54** 11169
[39] Perdew J P, Burke K and Ernzerhof M 1996 *Phys. Rev. Lett.* **77** 3865
[40] Blöchl P E 1994 *Phys. Rev. B* **50** 17953
[41] Kresse G and Joubert D 1999 *Phys. Rev. B* **59** 1758
[42] Momma K and Izumi F 2008 *J. Appl. Crystallogr* **41** 653
[43] Blundell S 2001 *Magnetism in Condensed Matter* (Oxford Master Series in Condensed Matter Physics) p. 145
[44] Kunstmann J, Özdoğan C, Quandt A and Fehske H 2011 *Phys. Rev. B* **83** 045414
[45] Lei S L, Li B, Huang J, Li Q X and Yang J L 2013 *Chin. Phys. Lett.* **30** 077502
[46] Ohta T, Bostwick A, Seyller T, Horn K and Rotenberg E 2006 *Science* **313** 951
[47] Feng W, Lei S L, Li Q X and Zhao A D 2011 *J. Phys. Chem. C* **115** 24858
[48] Chen J H, Li L, Cullen W G, Williams E D and Fuhrer M S 2011 *Nat. Phys.* **7** 535
[49] Nair R R, Tsai I L, Sepioni M, Lehtinen O, Keinonen J, Krasheninnikov A V, Castro Neto A H, Katsnelson M I, Geim A K and Grigorieva I V 2013 *Nat. Commun.* **4** 2010